AGU PUBLICATIONS

Global Biogeochemical Cycles

RESEARCH ARTICLE
10.1002/2016GB005520

Modeling radiocarbon constraints on the dilution of dissolved organic carbon in the deep ocean

Jamie D. Wilson[1] and **Sandra Arndt**[1,2]

[1] BRIDGE, School of Geographical Sciences, University of Bristol, Bristol, UK, [2] Department Geosciences, Environment and Society, Université Libre De Bruxelles, Brussels, Belgium

Key Points:
- A box model is used to explore the radiocarbon signature of diluted dissolved organic carbon in the deep ocean
- Modeled radiocarbon signature of diluted dissolved organic carbon can be reconciled with bulk observations within narrow parameter ranges
- Diluted DOC can alternatively be reconciled with a wide range of observations if it forms a small pool of radiocarbon-enriched DOC

Supporting Information:
- Supporting Information S1
- Data Set S1
- Data Set S2

Correspondence to:
J. D. Wilson,
jamie.wilson@bristol.ac.uk

Citation:
Wilson, J. D., and S. Arndt (2017), Modeling radiocarbon constraints on the dilution of dissolved organic carbon in the deep ocean, *Global Biogeochem. Cycles*, *31*, 775–786, doi:10.1002/2016GB005520.

Received 6 SEP 2016
Accepted 12 APR 2017
Accepted article online 19 APR 2017
Published online 4 MAY 2017

Abstract The recalcitrance of dissolved organic carbon (DOC) that leads to its accumulation in the deep ocean is typically considered a function of its reactivity. Yet, recent experimental evidence has shown that DOC from the deep ocean, if concentrated, can support significant microbial growth. This supports an alternative hypothesis that [DOC] may become too dilute to support microbial growth. The radiocarbon signature of DOC is a key constraint on the DOC cycling that allows testing of the plausibility of this hypothesis. Here we use a box model of diluted DOC in the deep ocean and its radiocarbon signature that is constrained on the basis of the new experimental evidence, as well as current knowledge of deep ocean DOC cycling to quantitatively test the dilution hypothesis. We explore the uncertainty in model results across a range of plausible dilution thresholds, additional processes, and fluxes of DOC to the deep ocean. Results show that the model is able to predict the observed radiocarbon signature for a dilution threshold close to the observed deep ocean [DOC] and for fluxes close to published estimates. Sensitivity analysis shows that this result is highly sensitive to variations in the dilution threshold and the assumption that diluted DOC is able to survive ocean overturning. The experimental findings can be alternatively reconciled over a large range of different conditions assuming a small pool of diluted DOC with a modern radiocarbon signature, consistent with recent observations, and offering a parsimonious interpretation of dilution with existing hypotheses on DOC recalcitrance.

1. Introduction

Dissolved organic carbon (DOC) forms the largest reservoir of organic carbon in the ocean with an inventory of 662 Pg C [*Hansell et al.*, 2009]. The majority of DOC in the ocean is formed by phytoplankton during photosynthesis (~21 Pg C yr^{-1}) with additional smaller sources from atmospheric deposition, rivers, and hydrothermal systems (all <0.36 Pg C yr^{-1}) [*Carlson and Hansell*, 2015]. Key features of ocean DOC cycling have previously been described using its radiocarbon signature ($\Delta^{14}C$) by the two-component model first proposed by *Williams and Druffel* [1987]. Observations show that both profiles of DOC concentration and $\Delta^{14}C$ decrease monotonically from the surface of the ocean before becoming almost uniform at depths >1000 m. The radiocarbon signature of surface ocean DOC, $\Delta^{14}C$, is depleted by ~300‰ relative to that of dissolved inorganic carbon (DIC), while deep ocean DOC (>1000 m) is generally characterized by bulk conventional radiocarbon ages of 4000 years in the Atlantic to 6000 years in the North Pacific ($\Delta^{14}C \sim -392‰$ to $-526‰$) [*Bauer et al.*, 1992]. Mass balance calculations and mixing models show that the consistent 300‰ depletion in surface waters can be explained by two distinct DOC pools: (1) a dynamic DOC pool that cycles on short timescales (10^{-1} to 10^{1} years) and is characterized by radiocarbon signatures close to that of DIC and (2) a well-mixed, radiocarbon depleted pool that cycles on the timescales of millennia [*Williams and Druffel*, 1987; *Beaupré and Aluwihare*, 2010].

A DOC pool that persists over millennial timescales in the deep ocean is central to the concept of the "microbial carbon pump" (MCP) [*Jiao et al.*, 2010, 2014]. Similar to the solubility, soft-tissue, and carbonate pumps that maintain a vertical gradient of DIC and alkalinity in the ocean against erosion by ocean circulation [*Volk and Hoffert*, 1985], the MCP is posited to maintain a gradient of DOC from short-lived, highly reactive DOC in the surface ocean to longer-lived, less reactive DOC in the deep ocean [*Legendre et al.*, 2015]. This gradient is supported by the production of structurally recalcitrant DOC, produced from the successive degradation of labile DOC in the surface ocean by marine microbes [*Legendre et al.*, 2015]. Changes in the production or

removal of recalcitrant DOC via the MCP could therefore exert an influence of atmospheric pCO_2 via changes in the size of the recalcitrant DOC pool [e.g., *Sexton et al.*, 2011; *Ridgwell and Arndt*, 2015].

A key question in this context is why DOC persists in the deep ocean for thousands of years. One leading hypothesis relates the persistence of this radiocarbon-depleted pool to its intrinsically recalcitrant molecular structure that prevents degradation by heterotrophic organisms [*Jiao et al.*, 2010; *Hansell*, 2013; *Benner and Amon*, 2015; *Dittmar*, 2015]. Although this hypothesis is supported by experimental evidence from incubation experiments [e.g., *Ogawa et al.*, 2001; *Koch et al.*, 2014], a large proportion of recalcitrant oceanic DOC remains unidentified [*Dittmar*, 2015]. In addition, the exact fate of such recalcitrant DOC in the deep ocean is still a matter of debate [*Legendre et al.*, 2015] and suggested sinks include photodegradation via UV irradiation in the surface ocean [*Mopper et al.*, 1991], interactions with sinking and suspended particles [*Druffel et al.*, 1998], and interactions with hydrothermal systems [*Hawkes et al.*, 2015].

An alternative explanation for the persistence of DOC in the deep ocean is that DOC is composed of a large diversity of molecules that bacteria could, in theory, degrade but that are present in concentrations that are too low to support the energetic requirements for uptake and degradation [*Jannasch*, 1994; *Dittmar*, 2015]. In a recent study, *Arrieta et al.* [2015a] provided experimental evidence in support of this alternative dilution hypothesis. Samples of seawater from the deep Pacific and Atlantic (1000 m to 4200 m) were spiked with in situ DOC to increase ambient DOC concentrations by a factor of 2, 5, and 10. *Arrieta et al.* [2015a] hypothesized that if DOC degradation were inherently limited by structural recalcitrance then no significant increase in bacterial growth should be observed in those samples during incubation. However, their incubation results revealed an increase in bacterial abundance and specific growth rates that were consistent with a Monod growth model. Monod models were fitted to the incubation data to infer an average concentration at which bacterial growth could no longer be supported, the so-called "dilution threshold." The mean dilution threshold across nine experiments was 30.7 ± 5.4 mmol m^{-3}, close to the lowest observed concentrations of DOC in the deep ocean of 34 mmol m^{-3}. *Arrieta et al.* [2015a] therefore suggest that the bioavailability of DOC in the deep ocean is primarily a function of dilution (i.e., concentration) rather than recalcitrant molecular structures.

Dilution and recalcitrant molecular structures are not mutually exclusive hypotheses. *Jiao et al.* [2014] recognize that DOC in the deep ocean may be composed of both a fraction that is intrinsically recalcitrant and a fraction that is bioavailable but cannot be degraded due to its low concentration. *Jiao et al.* [2015] alternatively suggest that bacterial growth observed in *Arrieta et al.* [2015a] was supported by a smaller bioavailable DOC fraction that was either present in the original DOC sample or was produced by processes such as viral lysis, chemolithoautotrophic activities, or grazing during the experiment rather than a release from dilution by enrichments . Furthermore, recent observations show that 8%–30% of DOC in the deep ocean possesses modern $\Delta^{14}C$ values (> −50‰) that would likely be associated with the heterotrophic degradation of sinking particulate organic carbon [*Follett et al.*, 2014; *Druffel et al.*, 2016; *Walker et al.*, 2016]. The remaining DOC in the deep ocean then has to be characterized by more depleted $\Delta^{14}C$ values than the bulk (e.g., −456‰ to −800‰), consistent with observations of significantly radiocarbon-depleted black carbon [*Ziolkowski and Druffel*, 2010].

Models are ideal tools to test the plausibility and robustness of a given hypothesis in a quantitative framework. Because the precise sources and sinks of DOC in the deep ocean are uncertain, a three-dimensional ocean biogeochemical model would be difficult to constrain and would thus offer few certain insights into the dynamics of a dilution-limited but bioavailable DOC pool. Constraining simpler mass balance models (box models) requires less data and mechanistic understanding. Such simple models still provide important insights into the dynamics of a deep ocean DOC pool and allow for the testing of key constraints on different hypotheses. The following key constraints are available to estimate $\Delta^{14}C$ of diluted, bioavailable DOC in the deep ocean: estimates of global DOC production [*Hansell*, 2013]; observations of the rate of DOC degradation by bacteria above a dilution threshold from *Arrieta et al.* [2015a]; and the volume of the deep ocean. To this end, a box model of dilution-limited but bioavailable DOC in the deep ocean is developed to assess the plausibility of dilution as a key driver of DOC persistence in the deep ocean. In addition, a sensitivity study is conducted over a wide range of plausible dilution thresholds and DOC input fluxes to the deep ocean to explore the robustness of model results. We explore whether the degradation rates are significant in a global context, whether a diluted DOC pool is consistent with observed $\Delta^{14}C$, and whether model results support alternative interpretations.

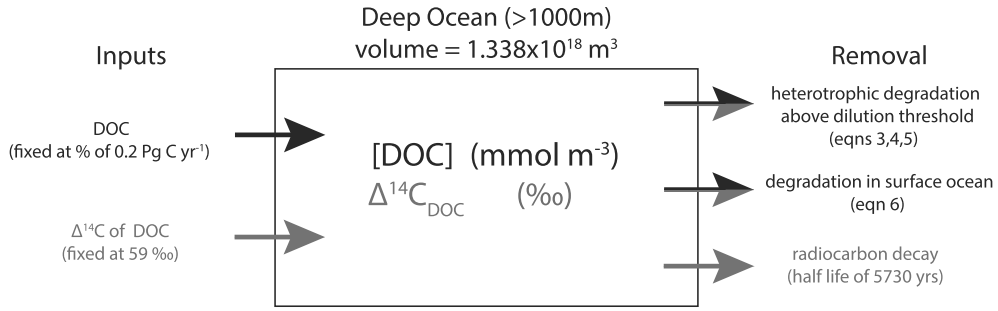

Figure 1. A schematic of the box model. The model predicts the concentration of DOC and isotopic ratio of radiocarbon for a given fixed production of DOC and associated radiocarbon ratio using degradation predicted by the uptake rates observed by *Arrieta et al.* [2015a] and removal on the timescale of upwelling to the surface ocean. Black and grey denote processes for DOC and radiocarbon, respectively.

2. Methods

2.1. Model Description

The conceptual model of deep ocean diluted DOC and its radiocarbon signature developed here is illustrated in Figure 1, and model parameter values are summarized in Table 1. Model code is provided in the supporting information.

The model comprises a single well-mixed box representing the global deep ocean below 1000 m where [DOC] is present at concentrations between ~34 mmol m^{-3} in the oldest waters of the deep North Pacific to ~45–50 mmol m^{-3} in the deep North Atlantic [*Hansell et al.*, 2009; *Hansell*, 2013]. The model explicitly accounts for a single pool of well-mixed, bioavailable, deep ocean DOC and predicts the concentration of this pool ([DOC]) and its ^{14}C signature (as the ratio between $^{14}C/^{12}C$) in response to the input flux of DOC and ^{14}C to the deep ocean, (F_{input}), as well as a number of characteristic removal processes ($\sum R$) (see sections 2.2 and 2.3 for details):

$$\frac{d[DOC]}{dt} = F_{input} - \sum R \quad (1)$$

$$\frac{d(^{14}C)}{dt} = {}^{14}C_{input} F_{input} - \sum {}^{14}CR - \lambda {}^{14}C[DOC] \quad (2)$$

The model is run to equilibrium to find a steady state solution for a set of given parameters.

2.2. Input Fluxes

2.2.1. DOC

The deep ocean box receives a constant input flux of bioavailable DOC, F_{input}, that represents photosynthetically derived organic matter which is considered the dominant source of DOC in the ocean [*Carlson and Hansell*, 2015]. F_{input} reflects a net input to the deep ocean (>1000 m), and we do not resolve the exact source, e.g., whether it is exported via ocean circulation or associated with the export of particulate organic carbon.

Table 1. Model Parameters, Values, Description, and Relevant References[a]

Symbols	Value	Description	Reference/Notes
v	1.338×10^{18} m^3	Volume of ocean >1000 m	*Menard and Smith* [1966]
F_{input}	variable; mol yr^{-1}	Input rate of DOC to the deep ocean	*Hansell* [2013]
R_{uptake}	variable; mmol m^{-3} yr^{-1}	Prokaryote uptake rate of DOC	*Arrieta et al.* [2015a]; see section 2.2.1
V_{max}	171.04 ± 161.70 mmol m^{-3} yr^{-1}	Maximum uptake rate of DOC	*Arrieta et al.* [2015a]; see section 2.3.1
K	231.16 ± 899.99 mmol m^{-3}	Half-saturation constant	*Arrieta et al.* [2015a]; see section 2.3.1
b	24.46 ± 89.83 mmol m^{-3} yr^{-1}	Maintenance coefficient	*Arrieta et al.* [2015a]; see section 2.3.1
$[DOC]_{min}$	38.6 ± 38.0 mmol m^{-3}	Dilution threshold for DOC	*Arrieta et al.* [2015a]
k	0 or 0.001 yr^{-1}	First-order decay constant	*Matsumoto* [2007]; see section 2.3.2
λ	1/8267 yr^{-1}	Radiocarbon decay constant	*Stuvier and Polach* [1977]

[a]Parameters from equation (3) are fitted by nonlinear regression and reported with 95% confidence intervals

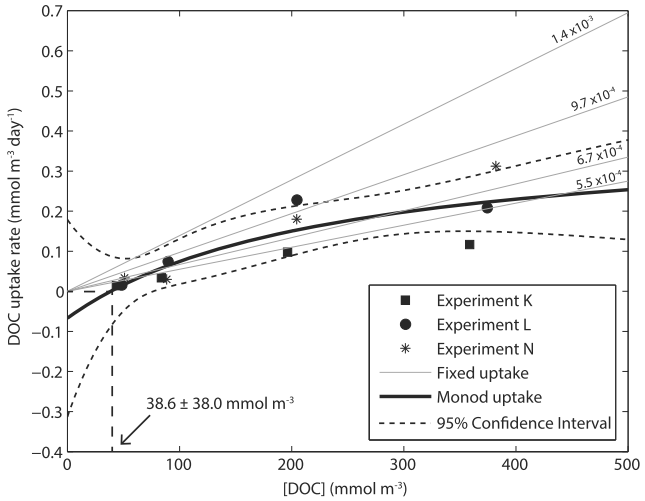

Figure 2. The Monod model used to predict DOC uptake rates above the dilution threshold (see equation (3)). The Monod model (black line) is fitted to the data available from *Arrieta et al.* [2015a] using nonlinear least squares regression. The 95% confidence interval for the fit is also shown (dashed lines). The concentration at which the fitted model predicts zero uptake is shown as 38.6 ± 38.0. The grey lines illustrate alternative estimates of DOC uptake calculated by *Arrieta et al.* [2015b] assuming a fixed specific substrate affinity of 1×10^{-11} L cell^{-1} d^{-1} and maximum prokaryote abundances indicated above each line in prokaryotes L^{-1}.

Note that because the input flux is constant, the model implies that the degradation of DOC in the deep ocean has no effect on the total production and export of DOC from the surface ocean. As the magnitude of the bioavailable DOC flux reaching the deep ocean is poorly constrained, F_{input} is varied systematically between 10% and 200% of the estimated DOC export to 500 m (0.2 Pg C yr^{-1}) [*Hansell*, 2013] to cover a wide range of plausible scenarios. The highest F_{input} value is consistent with the magnitude of POC fluxes at 2000m (0.43 Pg C yr^{-1} [*Honjo et al.*, 2008]). Although the export of DOC from the surface (1.5 Pg C yr^{-1} [*Hansell*, 2013]) is an absolute upper limit, we found that important details at lower fluxes were obscured and that results differed very little using fluxes above 0.2 Pg C yr^{-1}. We therefore choose 0.2 Pg C yr^{-1} as an upper limit.

2.2.2. $\Delta^{14}C_{DOC}$

It is assumed that the Δ^{14}C signature of the DOC input to the deep ocean reflects photosynthetically derived organic matter recently formed in the surface. The Δ^{14}C value corrects for the effect of fractionation during processes such as the formation of organic matter. The DOC input therefore inherits the area-weighted global mean Δ^{14}C of DIC for the modern surface ocean (0–100 m) calculated from the GLODAP data set [*Key et al.*, 2004], giving a value of 59 ± 51‰. Note that observations of radiocarbon include excess radiocarbon from nuclear bomb tests and so reflect modern values.

2.3. Removal Processes

2.3.1. Heterotrophic Degradation of DOC Above Dilution Threshold

Characteristic uptake rates of DOC by prokaryotes in the deep ocean are derived from the incubation experiments described in *Arrieta et al.* [2015a]. The net uptake of DOC is calculated from the DOC concentrations (mmol m^{-3}) reported at the beginning and end of three sets of incubation experiments (K, L, N; we adopt the same labeling of experiments from *Arrieta et al.* [2015a]) and converted to uptake rates by dividing the difference with the duration of each experiment to generate an average uptake rate (mmol m^{-3} d^{-1}). The data from experiment M is not considered here due to a second phase of growth being observed during the incubation [*Arrieta et al.*, 2015a]. The average uptake rates are estimated as a function of [DOC] on the basis of a Monod model used by *Arrieta et al.* [2015a]:

$$R_{uptake} = V_{max} \cdot \frac{[DOC]}{K + [DOC]} - b \quad (3)$$

where V_{max} denotes the maximum uptake rate (mmol m^{-3} d^{-1}), K is the half-saturation constant (mmol m^{-3}), and b is an intercept parameter (mmol m^{-3} d^{-1}) that allows the model to predict a zero uptake rate for a DOC concentration greater than 0. Parameters V_{max}, K, and b were derived by fitting equation (3) to the combined estimated uptake rates from experiments K, L, and N using nonlinear least squares regression (Figure 2 and

Table 1). The fitted model predicts uptake rates similar in magnitude to first-order rates alternatively calculated using an estimated substrate affinity by *Arrieta et al.* [2015b] (Figure 2). Parameters are reported in units of per year in Table 1 for consistency with other terms.

A dilution threshold ($[DOC]_{min}$) is calculated by solving equation (3) for [DOC] when R_{uptake}=0:

$$[DOC]_{min} = \frac{-bK}{b - V_{max}} \tag{4}$$

Our fit predicts that $R_{uptake} = 0$ for $[DOC]_{min}$=38.6 mmol m^{-3} (Figure 2) differing from the mean dilution threshold of 30.7 mmol m^{-3} found by *Arrieta et al.* [2015a] derived from fits to individual experiments that range from 10 mmol m^{-3} to 57 mmol m^{-3}. The 95% confidence interval on our fit shows that this variability could reflect uncertainty in the nonlinear fit to the data (Figure 2). For our fit, the lower limit for $[DOC]_{min}$ is 0 mmol m^{-3}, and the upper limit falls between 76 and 77 mmol m^{-3} giving errors of approximately ±38.0 mmol m^{-3}. In addition, as suggested by *Jiao et al.* [2015], the total concentrations of DOC in the experiment may reflect a mixture of recalcitrant DOC and bioavailable DOC that already existed in the control; e.g., bioavailable DOC may have made up 6% of the total DOC. As a consequence, the estimated dilution threshold derived on the basis of the Monod fit to total [DOC] concentrations may be overestimated. To explicitly explore the effect of uncertainty in the dilution threshold, we add a scaling term (x, unitless) into equation (3) that reflects the linear change in parameters when fitting equation (3) assuming that bacterial growth is supported by a smaller proportion of bioavailable DOC [*Jiao et al.*, 2015] (see Text S1 for a full derivation). This provides a way of scaling equation (3) for use with different dilution thresholds that is consistent with alternative interpretations of the data:

$$R_{uptake} = \begin{cases} V_{max} \cdot \frac{[DOC]}{Kx+DOC} - b, & \text{if } [DOC] \geq [DOC]^{new}_{min} \\ 0, & \text{otherwise} \end{cases} \tag{5}$$

where $x = \frac{[DOC]^{new}_{min}}{[DOC]_{min}}$.

2.3.2. Degradation of Deep-Water DOC in the Surface Ocean

A second removal term is included in the model to represent the consumption of DOC via upwelling and degradation (heterotrophic degradation and/or photochemical degradation) in the surface ocean. We do not explicitly resolve ocean circulation and surface ocean consumption processes in this model. Instead, we include a first-order consumption term that assigns DOC a deep ocean lifetime that equals the timescale of ocean overturning [e.g., *Anderson et al.*, 2015]:

$$R_{overturning} = k \cdot [DOC] \tag{6}$$

where k is a first-order rate constant (yr^{-1}) that is constrained by the characteristic residence time of water in the deep ocean of approximately 1000 years [*Matsumoto*, 2007] (Table 1).

2.3.3. Removal of Radiocarbon

Deep ocean ^{14}C is consumed during the degradation of DOC but is not fractionated during these processes; i.e., it is removed at the same isotopic ratio. In addition, ^{14}C also decays with a half-life of 5730 years (λ = 1/8267 yr^{-1}, equation (2)) [*Stuvier and Polach*, 1977].

2.4. Experiments

We explore the simulated steady state deep ocean DOC concentration and its Δ^{14}C signature for three sets of experiments:

1. *Testing the plausibility of the dilution hypothesis according to Arrieta et al.* [2015a]: We first use the model to explore a hypothetical scenario where DOC that is available for uptake by prokaryotes in the deep ocean is limited by dilution only; i.e., the first-order reaction rate term in the model (k) is set to 0. The dilution threshold is constrained on the basis of experimental results (DOC_{min}= 38.6 ± 38.0 mmol m^{-3}) to explicitly test whether the hypothesis of *Arrieta et al.* [2015a] is consistent with observations of Δ^{14}C in the deep ocean.
2. *Testing the robustness of model results*: The dilution threshold found by *Arrieta et al.* [2015a] is an average of values ranging from 10 to 57 mmol m^{-3} that may reflect some unknown variability in the data [*Jiao et al.*, 2015] or equal uncertainty in the fitting of the Monod function as demonstrated in Figure 2. Therefore, we test the robustness of the model results for a range of different dilution thresholds ($[DOC]_{min}$= 10 to 42 mmol m^{-3}).

3. *Testing the sensitivity of the model to the assumption that dilution is the key removal process*: Lastly, we explore a scenario where dilution-limited DOC is removed from the deep ocean with ocean overturning. If concentration is the key limiting factor for heterotrophic degradation, then we may expect that upwelled DOC is bioavailable and will be degraded in the surface ocean where concentrations are much higher, potentially violating the observation that deep ocean DOC is uniformly distributed throughout the water column [*Williams and Druffel*, 1987]. In addition, DOC in the surface ocean will be subject to photodegradation. To explore this, we set the additional first-order degradation rate (equation (6)) to reflect an average lifetime of water in the deep ocean of approximately 1000 years (*k*: Table 1) [*Matsumoto*, 2007]. Note that in the model, deep ocean DOC above the dilution threshold is still consumed by heterotrophic degradation but it now has an upper limit to its lifetime in the deep ocean.

Because the magnitude of the DOC input to the deep ocean, F_{input}, is uncertain, we systematically explore the results across a range between 10% and 200% of global DOC export to 500m suggested by *Hansell* [2013] in all experiments.

3. Results

3.1. Dilution-Limited Degradation of DOC

Model results show that across the range of tested DOC input fluxes F_{input}, deep ocean DOC concentrations are maintained within 1 mmol m^{-3} of the dilution threshold of 38.6 mmol m^{-3} (Figure S3). This finding is robust if V_{max} is reduced by an order of magnitude, as well as if the input flux is increased to the estimated export of DOC from the surface ocean (1.9 Pg C yr^{-1} [*Hansell*, 2013]). Model results thus show that heterotrophic degradation rates of DOC in the deep ocean could maintain DOC concentrations close to the dilution threshold, mainly because the input rate of DOC to the the large deep ocean reservoir (volume = 1.338×10^{18} m^3) is relatively small in comparison to the degradation rate (0.01×10^{-2} to 2.49×10^{-2} mmol m^{-3} yr^{-1}; cf. maximum uptake rate of 171.04 mmol m^{-3} yr^{-1}). Therefore, the degradation rates inferred from the experiments of *Arrieta et al.* [2015a] are significant in the context of global DOC cycling in the deep ocean [*Jiao et al.*, 2015; *Arrieta et al.*, 2015b].

Yet the model indicates that the radiocarbon signature $\Delta^{14}C$ of the deep ocean DOC pool is sensitive to the influx of DOC to the deep ocean (Figure 3). $\Delta^{14}C$ becomes more depleted with smaller input fluxes. Low DOC input to the deep ocean leads to a longer residence time of DOC in the deep ocean, and, as a consequence, radiocarbon decay depletes ^{14}C. At higher input fluxes, deep ocean DOC concentrations increase at a faster rate leading to an increase in the prokaryote degradation rates and therefore a more rapid turnover of DOC. The $\Delta^{14}C$ and inferred input fluxes are robust to the uncertainty in radiocarbon signature of the input flux (dashed lines in Figure 3).

Model results show that it is possible to find $\Delta^{14}C$ values that are close to the bulk observed $\Delta^{14}C$ of −392‰ to −526‰ at a dilution threshold of 38.6 mmol m^{-3} (Figure 3), thus suggesting that the dilution hypothesis can, under certain conditions, be reconciled with radiocarbon observations. In our model this requires DOC input fluxes to the deep ocean of between 0.062 and 0.102 Pg C yr^{-1}. The lower part of this range is consistent with a previous model estimate of 0.043 Pg C yr^{-1} for recalcitrant DOC production, derived from modeled DOC production, observed removal rates, and the misfit between model and observed [DOC] fields [*Hansell et al.*, 2012]. The $\Delta^{14}C$ is slightly sensitive to the $\Delta^{14}C$ of the input. Varying this within 1 standard deviation gives a total range of 0.057 to 0.114 Pg C yr^{-1}. Therefore, a modeled dilution-limited DOC pool in the deep ocean can produce $\Delta^{14}C$ values consistent with observations at a plausible rate of input to the deep ocean. However, we note that the model predicts that the degradation rates are 0.1 to 0.2 mmol m^{-3} yr^{-1} which are 2 orders of magnitude larger than degradation rates in the deep ocean estimated from DOC observations (0.004 µmol kg^{-1} yr^{-1} [*Hansell et al.*, 2012]) and that the tested dilution threshold is slightly higher than the lowest observed concentrations in the deep ocean (~34 mmol m^{-3}).

3.2. Sensitivity to Uncertainty in Dilution Thresholds

Figure 4a shows how the concentration of DOC varies as a function of both the DOC input flux and now the dilution threshold. As with the previous set of experiments, deep ocean DOC is always maintained close to the dilution threshold, as indicated by the horizontal contour lines; i.e., for a given dilution threshold, deep ocean DOC concentrations remain within 1 mmol m^{-3} across the entire range of assumed DOC input fluxes.

In addition, model results show that $\Delta^{14}C$ is sensitive to both the DOC input flux and the dilution threshold (Figure 4b). As before, $\Delta^{14}C$ becomes less depleted with higher input fluxes. In addition, lower dilution

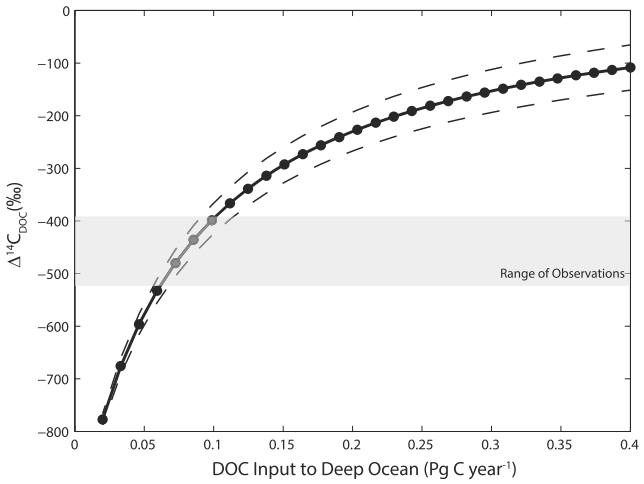

Figure 3. Steady state model results for $\Delta^{14}C$ at different DOC input fluxes with an explicit dilution-limited DOC pool tested for the dilution threshold of 38.6 mmol m^{-3} from the fit to incubation experiments in Figure 2. Dashed lines indicate the 1 standard deviation uncertainty in the mean $\Delta^{14}C$ of the DOC input flux. Each circle is a steady state solution for $\Delta^{14}C$ for a given DOC input flux. The grey shading indicates the range of $\Delta^{14}C$ values in the deep ocean for comparison.

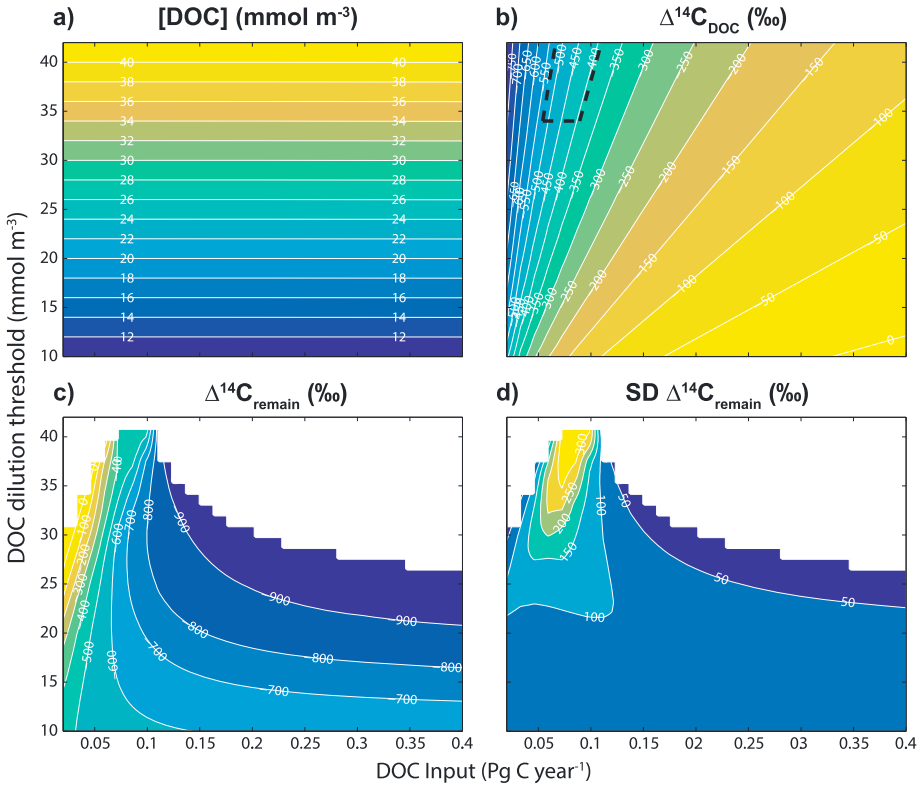

Figure 4. Steady state model results for DOC and $\Delta^{14}C$ with an explicit dilution-limited DOC pool tested over a range of DOC input fluxes and dilution thresholds. (a) Contours of the predicted concentration of DOC, (b) contours of the predicted $\Delta^{14}C$. The area within the dashed lines represents the range of $\Delta^{14}C$ observed in the deep ocean (392‰ to 526‰). (c) Contours of mean $\Delta^{14}C$ calculated from mass balance (see equation (7)) tested across a range of assumptions and (d) the standard deviation of $\Delta^{14}C$ in Figure 4c. White areas in Figures 4c and 4d indicate where $\Delta^{14}C$ is >150‰ or < −1000‰.

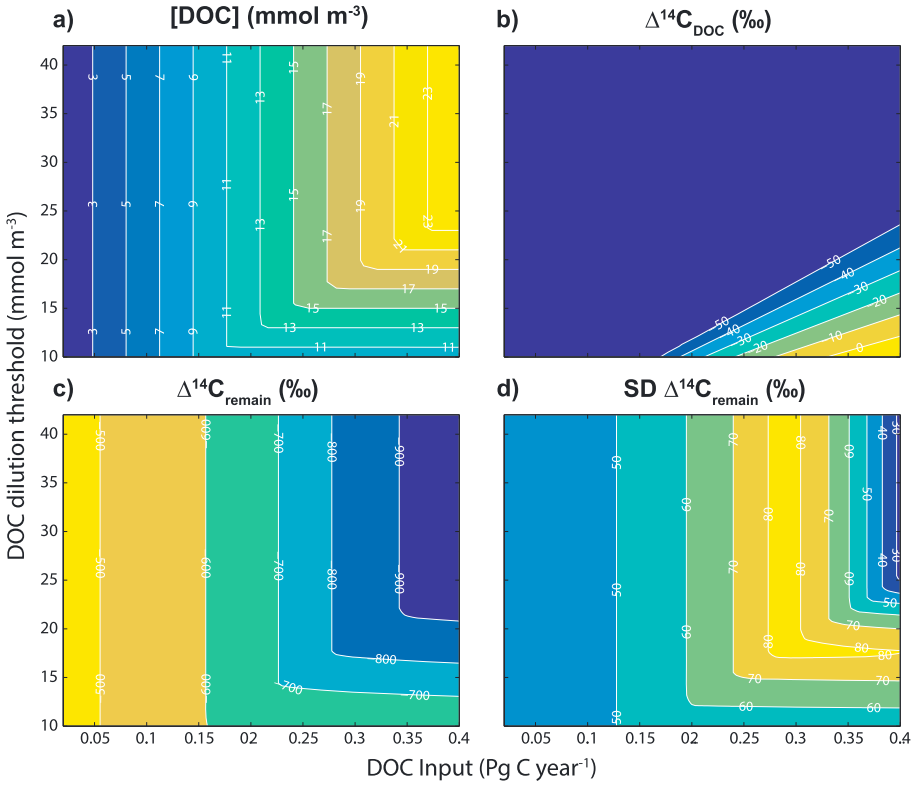

Figure 5. Steady state model results for DOC and $\Delta^{14}C$ with a dilution-limited DOC pool with additional degradation occurring on the timescale of ocean overturning. (a) Contours of the predicted concentration of DOC, (b) contours of the predicted $\Delta^{14}C$. (c) Contours of mean $\Delta^{14}C$ calculated from mass balance (see equation (7)) tested across a range of assumptions and (d) the standard deviation of $\Delta^{14}C$ in Figure 5c.

thresholds also result in lower $\Delta^{14}C$ because deep ocean DOC concentrations close to the dilution threshold are quickly reached resulting in a lower residence time. Notably, a large fraction of the parameter space is associated with $\Delta^{14}C$ that is less depleted than observed (Figure 4b) indicating that the dilution hypothesis can only be reconciled with available radiocarbon constraints for a narrow range of dilution thresholds ($DOC_{min} \approx$ 34 to 42 mmol m^{-3}) and deep ocean DOC input ($F_{in} \approx 0.05$ to 0.1 Pg C yr^{-1}) (see Figure 4b indicated by dashed line), indicating that reactivity might be a more likely explanation for DOC persistence in the deep ocean .

However, as discussed earlier, dilution and recalcitrant molecular structures are not mutually exclusive explanations for the persistence of deep ocean DOC. One could imagine a bioavailable but dilution-limited DOC pool, $[DOC]_{diluted}$, that represents a small fraction of the total deep ocean, $[DOC]_{bulk}$. Its radiocarbon signature $\Delta^{14}C$ is a small component of the average $\Delta^{14}C$ values of the total pool, and the dilution hypothesis could thus be reconciled with radiocarbon observations over a wider range of different dilution thresholds and deep ocean DOC fluxes. We therefore use mass balance (equation (7)) to explore what $\Delta^{14}C$ values of the remaining DOC pool and $\Delta^{14}C$ are required to match the bulk $\Delta^{14}C$ between −392‰ and −526‰.

$$\Delta^{14}C_{remain} = \frac{[DOC]_{bulk}\Delta^{14}C_{bulk} - [DOC]_{diluted}\Delta^{14}C_{diluted}}{[DOC]_{remain}} \quad (7)$$

To cover the range of observed deep ocean $[DOC]_{bulk}$ and $\Delta^{14}C_{bulk}$, we generate 1000 randomly sampled $[DOC]_{bulk}$ and $\Delta^{14}C_{bulk}$ couples within a range of 34 to 42 mmol m^{-3} and −392 and −526‰, respectively. Figure 4c illustrates the resulting mean $\Delta^{14}C_{remain}$, and 1 standard deviation of these mass balance calculations is shown in Figure 4d. Figure 4c shows that there is a wide range of $[DOC]_{remain}$ and $\Delta^{14}C_{remain}$ combinations for which simulated DOC and $\Delta^{14}C_{bulk}$ cannot be reconciled with observations because it would require unrealistic $\Delta^{14}C_{remain}$ values of >150‰ or < −1000‰ (radiocarbon dead). These results are robust to choice of [DOC] and $\Delta^{14}C_{bulk}$ (Figure 4d).

Figure 4c shows that for most dilution thresholds, the $\Delta^{14}C_{remain}$ required to match observations are similar to the observed deep ocean $\Delta^{14}C$ or older. In other words, we would either require a recalcitrant and diluted DOC pool with similar $\Delta^{14}C$ values to each other or a bioavailable but diluted pool with $\Delta^{14}C$ values close to modern (−100‰ to 0‰) and a recalcitrant pool with values that are more depleted (< −600‰).

3.3. Sensitivity to Additional DOC Consumption on the Timescale of Ocean Overturning

The additional removal of dilution-limited deep ocean DOC by ocean overturning and consumption in the surface ocean results in simulated deep ocean DOC concentrations below the dilution threshold across the parameter space (Figure 5a). DOC in the model is still available to be removed over a given dilution threshold but now has an upper limit to its lifetime in the deep ocean. Model results show that deep ocean DOC concentrations are mainly controlled by input fluxes. At low input fluxes, consumption processes maintain deep ocean DOC concentrations at very low levels (<11 mmol m^{-3}) across the full range of dilution thresholds tested (vertical contours in Figure 5a). As DOC input fluxes increase (> 0.2 Pg C yr^{-1}), deep ocean DOC concentrations reach the dilution threshold and are maintained close to this threshold in a similar way to the dilution-only scenario (cf. Figures 5a and 4a). The strong control of DOC input fluxes on deep ocean DOC simulated here indicates that the results of the dilution-only scenario and, in particular, the strong link between deep ocean DOC and dilution threshold require that the diluted DOC is not consumed in the surface ocean (i.e., its ability to undergo multiple cycles of ocean overturning).

The model predicts a constant $\Delta^{14}C$ value of −55‰ for diluted DOC across most of the parameter space (Figure 5b). Because deep ocean DOC concentrations fall below the dilution thresholds, DOC is merely consumed by the additional consumption processes. Process rates are controlled by the constant, first-order degradation rate constant k, and the residence time of the DOC is thus also constant. $\Delta^{14}C$ values become less depleted for high input fluxes that result in deep ocean DOC concentrations above the dilution thresholds.

Repeating the same mass balance calculation as in the previous experiments shows that the much less depleted $\Delta^{14}C$ of the simulated DOC pool can easily be reconciled with the bulk DOC pool. In this experiment, the diluted DOC constitutes only a small fraction of the bulk DOC pool (Figure 5c). All $\Delta^{14}C$ values are close to or more depleted than the observed value in the deep North Pacific of ∼ −526‰. Again, these results are relatively robust to choice of [DOC] and $\Delta^{14}C$ (Figure 5d).

4. Discussion

4.1. Reconciling Model Results and Observations

The growth of prokaryotes and the consumption of deep ocean DOC when concentrated challenges the hypothesis that heterotrophic degradation of DOC in the ocean is limited by the recalcitrant nature of deep ocean DOC and indicates that dilution limits heterotrophic activity and leads to the persistence of DOC in the deep ocean [*Arrieta et al.*, 2015a]. We have presented a set of box model experiments to test the plausibility of the dilution hypothesis as supported by recent experimental evidence and explore whether a dilution-limited pool of DOC in the deep ocean is consistent with $\Delta^{14}C$ observations. Model results suggest that there are, in theory, two plausible interpretations of the experimental results presented by *Arrieta et al.* [2015a] that are consistent with $\Delta^{14}C$ observations: (1) dilution limits the heterotrophic degradation of DOC in the deep ocean or (2) dilution-limited DOC forms a relatively small fraction of the total deep ocean DOC which is cycled relatively rapidly. We find that the observations of uptake rates for DOC by prokaryotes are significant enough to maintain a pool of DOC at a dilution threshold and produce $\Delta^{14}C$ values that are within the range of observed values for the deep ocean for a dilution threshold close to the observed concentration of DOC in the deep ocean and fluxes consistent with modeling and data estimates.

However, model results also show that the dilution hypothesis can only be reconciled with available radiocarbon constraints for a narrow range of dilution thresholds (DOC_{min} ≈ 34 to 42 mmol m^{-3}) and deep ocean DOC input (F_{in} ≈ 0.05 to 0.1 Pg C yr^{-1}) couples. In addition, the results of the dilution-only scenario and, in particular, the strong link between deep ocean DOC and dilution threshold are sensitive to key assumptions, alternatively suggesting that bioavailable but diluted DOC could form a smaller fraction of the total deep ocean DOC, either because of a lower dilution threshold and/or because it is limited by degradation in the surface ocean, with a relatively enriched $\Delta^{14}C$ signature.

Given the observations of *Arrieta et al.* [2015a] and basic constraints on DOC cycling in the deep ocean, our model can estimate $\Delta^{14}C$ at global fluxes matching model and data estimates (Figure 3) providing support

for dilution as a mechanism explaining the persistence of DOC in the deep ocean. However, this solution may arise for other reasons. The depletion of radiocarbon reflects the average time of DOC in the deep ocean, or the residence time (τ). In the case of a system at steady state, such as our model, this is equal to the quotient between concentration (M) and flux in or out (F) of the system: $\tau = \frac{M}{F}$. Because the uptake rates observed by *Arrieta et al.* [2015a] are sufficient to maintain the concentration of DOC at the dilution threshold close to the observed concentration and we are looking to find the observed $\Delta^{14}C$, it therefore follows that we find a flux similar in magnitude to other studies, e.g., *Hansell et al.* [2012]. We therefore need to explore whether this interpretation is consistent with other observations.

There is increasing evidence that the observed $\Delta^{14}C$ for DOC in the deep ocean represents an average of a plethora of different $\Delta^{14}C$ values ranging from −918‰ [*Ziolkowski and Druffel*, 2010] to bomb radiocarbon ($\Delta^{14}C > -50$‰) [*Follett et al.*, 2014; *Druffel et al.*, 2016; *Walker et al.*, 2016]. The range of values suggests that there multiple pools of DOC in the deep ocean that cycle at different timescales. For example, the presence of bomb radiocarbon in the deep ocean that has been estimated to represent up to 8–10% of total DOC in the North Atlantic [*Druffel et al.*, 2016] and up to 30% in the central Pacific Ocean [*Follett et al.*, 2014] suggests that the hydrolysis of sinking POC is a source of deep ocean DOC. In addition, DOC relatively enriched in $\Delta^{14}C$ is also associated with high molecular weight in a relationship consistent with reactivity [*Walker et al.*, 2016]. A predominantly bioavailable but diluted DOC pool in the deep ocean would be hard to reconcile with these observations.

Model results indicate that relationship between prokaryote uptake rates and concentration observed by *Arrieta et al.* [2015a] can be more easily reconciled with observations if they are related to a much smaller dilution threshold and/or significant removal in the surface ocean. These results are also consistent with the magnitude of fluxes associated with POC as a source for this DOC. We therefore suggest that the parsimonious interpretation of the results of *Arrieta et al.* [2015a] is that they reflect the presence of a small fraction of bioavailable DOC in the deep ocean rather than indicative of dilution as a key mechanism. This result is also parsimonious with a relationship between molecular size and reactivity [*Walker et al.*, 2016], the existence of a persistent, slowly cycled pool of DOC that is uniformly distributed through the water column [*Williams and Druffel*, 1987; *Beaupré and Aluwihare*, 2010], and the potential for the microbial carbon pump to sequester CO_2 [*Jiao et al.*, 2010, 2014].

4.2. Further Work

4.2.1. Observations

The findings of *Arrieta et al.* [2015a] have suggested that bioavailable DOC exists in the deep ocean, but further work is needed to elucidate the source, inventory, and significance of this DOC. Mass balance calculations of ^{14}C measurements at the beginning and end of an experimental setup similar to that of *Arrieta et al.* [2015a] could help further distinguish between the two model scenarios presented in this paper. For example, relatively enriched $\Delta^{14}C$ for the DOC consumed during incubations would add strong evidence toward a smaller sized bioavailable DOC pool. Such an approach would need to consider the variability in ^{14}C ages that has been previously observed across different size classes of DOC, with age increasing inversely with size [*Guo et al.*, 1996], as well as across different compounds [*Aluwihare et al.*, 2002; *Loh et al.*, 2004; *Repeta and Aluwihare*, 2006].

4.2.2. Modeling

Although the model we have applied here is relatively simplistic and conceptual, it demonstrates that there are a number of basic constraints on DOC cycling in the deep ocean. However, there are key caveats to the results presented that relate to the representation of DOC and the resolution of the model. First, bioavailable DOC in our model is represented as a single pool in a similar way that ocean biogeochemical models commonly represent DOC as distinct pools with varying characteristic decay rates [see *Anderson et al.*, 2015]. In contrast, the dilution hypothesis posits that it is the concentration of the diverse individual DOC compounds that are limiting [*Jannasch*, 1994; *Dittmar*, 2015; *Arrieta et al.*, 2015a]. Other key factors that may also be important to consider in terms of the bioavailability of DOC include the biomass of consuming organisms, their ability to produce specific exoenzymes or their requirements for specific compounds, and environmental conditions. In this context, our box model represents a scenario where all compounds are equally available, or at least available in fixed ratios, and consumers are always present and able to consume once concentrations are high enough. An alternative approach that explicitly includes these factors may increase our estimates of

^{14}C-based ages of diluted DOC in the deep ocean and exacerbate the key constraints we have identified with our box model.

Constraining the dynamics of diluted DOC in the deep ocean and the associated potential for multiple cycles of DOC further, as well as the implications for the microbial carbon pump, ideally requires a model with 3-D resolution to resolve the spatial patterns of ocean circulation and biological activity. This may be particularly important if diluted DOC is linked to processes such as POC fluxes which are spatially and temporally variable. However, this requires further observations of diluted DOC with which to validate the model. If the solubilization of POC is a key source for diluted DOC, then we should expect to observe nonconservative behavior in bulk DOC consistent with the spatial variability in POC [*Follett et al.*, 2014] as well as changes in Δ^{14}C through time associated with changes in bomb radiocarbon in the atmosphere and surface ocean. Further work building on nonconservative behavior in observations [e.g., *Hansell and Carlson*, 2013; *Follett et al.*, 2014; *Bercovici and Hansell*, 2016] may be therefore required to help constrain a model with a 3-D resolution. Finally, another challenge for incorporating the dilution and dynamic cycling of DOC into more complex biogeochemical models is developing a mechanistic representation that includes both the controls of dilution and structural recalcitrance as limits on the degradation of DOC. One potential approach may be to explicitly model the cycling of DOC using the relationship between molecular size and reactivity [e.g., *Walker et al.*, 2016]. Such an approach could link diluted DOC in the deep ocean directly to POC fluxes and would provide a mechanistic model with which to explore the dynamics of a microbial carbon pump.

5. Conclusions

The dilution of DOC below a dilution threshold has been posited as an explanation for the apparent persistence of DOC in the deep ocean *Arrieta et al.* [2015a]. We have presented a box model of dilution-limited DOC in the deep ocean that uses observed prokaryote uptake rates of concentrated DOC from *Arrieta et al.* [2015a] to explore whether this is consistent with observed Δ^{14}C and the constraints it places on DOC cycling. Although it is possible to predict observed Δ^{14}C using the model at magnitudes of production similar to previously predicted, this result is very sensitive to the accuracy of the dilution threshold estimate and the assumption that there are no significant removal processes occurring such as degradation in the surface ocean. Our model suggests that taking these uncertainties into account results in a pool of diluted DOC that is rapidly turned over producing near modern Δ^{14}C values and which makes up a small proportion of the total DOC in the deep ocean. We suggest that this result is most consistent with the range of observations in the ocean providing a parsimonious interpretation of diluted DOC and hypotheses surrounding reactivity. Ultimately, the presence of diluted DOC in the deep ocean suggests the possibility that cycling of DOC is more complex requiring further work to elucidate the sources and sinks of bioavailable DOC and a modeling approach that can accommodate the various controls on DOC cycling.

Acknowledgments
J.D.W. acknowledges funding from the EU grant ERC-2013-CoG-617313. S.A. is supported by funding from the European Unions Horizon 2020 research and innovation program under the Marie Skłodowska-Curie grant agreement 643052. The data used in this paper were obtained freely from http://digital.csic.es/handle/10261/111563. Model code is available in the supporting information. We would like to thank Jesús Arrieta and colleagues for making their data freely available as well as thank three anonymous reviewers and the Editor for their constructive comments.

References

Aluwihare, L. I., D. J. Repeta, and R. F. Chen (2002), Chemical composition and cycling of dissolved organic matter in the Mid-Atlantic Bight, *Deep Sea Res., Part II*, *49*(20), 4421–4437, doi:10.1016/S0967-0645(02)00124-8.

Anderson, T. R., J. R. Christian, and K. J. Flynn (2015), Modeling DOM biogeochemistry, in *Biogeochemistry of Marine Dissolved Organic Matter*, edited by D. A. Hansell and and C. A. Carlson, pp. 717–755, Academic Press, San Diego, Calif.

Arrieta, J. M., E. Mayol, R. L. Hansman, G. J. Herndl, T. Dittmar, and C. M. Duarte (2015a), Dilution limits dissolved organic carbon utilization in the deep ocean, *Science*, *348*(6232), 331–333, doi:10.1126/science.1258955.

Arrieta, J. M., E. Mayol, R. L. Hansman, G. J. Herndl, T. Dittmar, and C. M. Duarte (2015b), Response to comment on "Dilution limits dissolved organic carbon utilization in the deep ocean", *Science*, *350*(6267), 1483–1483, doi:10.1126/science.aac7249.

Bauer, J. E., P. M. Williams, and E. R. M. Druffel (1992), ^{14}C activity of dissolved organic carbon fractions in the north-central Pacific and Sargasso Sea, *Nature*, *357*(6380), 667–670, doi:10.1038/357667a0.

Beaupré, S., and L. Aluwihare (2010), Constraining the 2-component model of marine dissolved organic radiocarbon, *Deep Sea Res., Part II*, *57*(16), 1494–1503, doi:10.1016/j.dsr2.2010.02.017.

Benner, R., and R. M. Amon (2015), The size-reactivity continuum of major bioelements in the ocean, *Annu. Rev. Mar. Sci.*, *7*(1), 185–205, doi:10.1146/annurev-marine-010213-135126.

Bercovici, S. K., and D. A. Hansell (2016), Dissolved organic carbon in the deep Southern Ocean: Local versus distant controls, *Global Biogeochem. Cycles*, *30*(2), 350–360, doi:10.1002/2015GB005252.

Carlson, C., and D. Hansell (2015), DOM sources, sinks, reactivity, and budgets, in *Biogeochemistry of Marine Dissolved Organic Matter*, edited by D. Hansell and and C. Carlson, pp. 65–126, Academic Press, Boston, Mass.

Dittmar, T. (2015), Reasons behind the long-term stability of dissolved organic matter, in *Biogeochemistry of Marine Dissolved Organic Matter*, edited by D. Hansell and and C. Carlson, pp. pp. 369–388, Academic Press, Boston, Mass.

Druffel, E., S. Griffin, J. Bauer, D. Wolgast, and X.-C. Wang (1998), Distribution of particulate organic carbon and radiocarbon in the water column from the upper slope to the abyssal NE Pacific Ocean, *Deep Sea Res., Part II*, *45*(4-5), 667–687, doi:10.1016/S0967-0645(98)00002-2.

Druffel, E. R. M., S. Griffin, A. I. Coppola, and B. D. Walker (2016), Radiocarbon in dissolved organic carbon of the Atlantic Ocean, *Geophys. Res. Lett.*, doi:10.1002/2016GL068746.

Follett, C. L., D. J. Repeta, D. H. Rothman, L. Xu, and C. Santinelli (2014), Hidden cycle of dissolved organic carbon in the deep ocean, *Proc. Natl. Acad. Sci. U.S.A.*, *111*(47), 16,706–16,711, doi:10.1073/pnas.1407445111.

Guo, L., P. H. Santschi, L. A. Cifuentes, S. E. Trumbore, and J. Southon (1996), Cycling of high-molecular-weight dissolved organic matter in the Middle Atlantic Bight as revealed by carbon isotopic (^{13}C and ^{14}C) signatures, *Limnol. Oceanogr.*, *41*(6), 1242–1252, doi:10.4319/lo.1996.41.6.1242.

Hansell, D., C. Carlson, D. Repeta, and R. Schlitzer (2009), Dissolved organic matter in the ocean: A controversy stimulates new insights, *Oceanography*, *22*(4), 202–211.

Hansell, D. A. (2013), Recalcitrant dissolved organic carbon fractions, *Annu. Rev. Mar. Sci.*, *5*(1), 421–445, doi:10.1146/annurev-marine-120710-100757.

Hansell, D. A., and C. A. Carlson (2013), Localized refractory dissolved organic carbon sinks in the deep ocean, *Global Biogeochem. Cycles*, *27*(3), 705–710, doi:10.1002/gbc.20067.

Hansell, D. A., C. A. Carlson, and R. Schlitzer (2012), Net removal of major marine dissolved organic carbon fractions in the subsurface ocean, *Global Biogeochem. Cycles*, *26*, GB1016, doi:10.1029/2011GB004069.

Hawkes, A., et al. (2015), Efficient removal of recalcitrant deep-ocean dissolved organic matter during hydrothermal circulation, *Nat. Geosci.*, *8*(11), 856–860.

Honjo, S., S. J. Manganini, R. A. Krishfield, and R. Francois (2008), Particulate organic carbon fluxes to the ocean interior and factors controlling the biological pump: A synthesis of global sediment trap programs since 1983, *Prog. Oceanogr.*, *76*(3), 217–285, doi:10.1016/j.pocean.2007.11.003.

Jannasch, H. W. (1994), The microbial turnover of carbon in the deep-sea environment, *Global Planet. Change*, *9*(3), 289–295, doi:10.1016/0921-8181(94)90022-1.

Jiao, N., G. J. Herndl, D. A. Hansell, R. Benner, G. Kattner, S. W. Wilhelm, D. L. Kirchman, M. G. Weinbauer, T. Luo, F. Chen, and F. Azam (2010), Microbial production of recalcitrant dissolved organic matter: Long-term carbon storage in the global ocean, *Nat. Rev. Microbiol.*, *8*(8), 593–599.

Jiao, N., et al. (2014), Mechanisms of microbial carbon sequestration in the ocean—Future research directions, *Biogeosciences*, *11*(19), 5285–5306, doi:10.5194/bg-11-5285-2014.

Jiao, N., et al. (2015), Comment on "Dilution limits dissolved organic carbon utilization in the deep ocean", *Science*, *350*(6267), 1483–1483, doi:10.1126/science.aab2713.

Key, R. M., A. Kozyr, C. L. Sabine, K. Lee, R. Wanninkhof, J. L. Bullister, R. A. Feely, F. J. Millero, C. Mordy, and T.-H. Peng (2004), A global ocean carbon climatology: Results from Global Data Analysis Project (GLODAP), *Global Biogeochem. Cycles*, *18*, GB4031, doi:10.1029/2004GB002247.

Koch, B. P., G. Kattner, M. Witt, and U. Passow (2014), Molecular insights into the microbial formation of marine dissolved organic matter: Recalcitrant or labile?, *Biogeosciences*, *11*(15), 4173–4190, doi:10.5194/bg-11-4173-2014.

Legendre, L., R. B. Rivkin, M. G. Weinbauer, L. Guidi, and J. Uitz (2015), The microbial carbon pump concept: Potential biogeochemical significance in the globally changing ocean, *Prog. Oceanogr.*, *134*, 432–450, doi:10.1016/j.pocean.2015.01.008.

Loh, A. N., J. E. Bauer, and E. R. M. Druffel (2004), Variable ageing and storage of dissolved organic components in the open ocean, *Nature*, *430*(7002), 877–881.

Matsumoto, K. (2007), Radiocarbon-based circulation age of the world oceans, *J. Geophys. Res.*, *112*, C09004, doi:10.1029/2007JC004095.

Menard, H. W., and S. M. Smith (1966), Hypsometry of ocean basin provinces, *J. Geophys. Res.*, *71*(18), 4305–4325, doi:10.1029/JZ071i018p04305.

Mopper, K., X. Zhou, R. J. Kieber, D. J. Kieber, R. J. Sikorski, and R. D. Jones (1991), Photochemical degradation of dissolved organic carbon and its impact on the oceanic carbon cycle, *Nature*, *353*(6339), 60–62.

Ogawa, H., Y. Amagai, I. Koike, K. Kaiser, and R. Benner (2001), Production of refractory dissolved organic matter by bacteria, *Science*, *292*(5518), 917–920, doi:10.1126/science.1057627.

Repeta, D. J., and L. I. Aluwihare (2006), Radiocarbon analysis of neutral sugars in high-molecular-weight dissolved organic carbon: Implications for organic carbon cycling, *Limnol. Oceanogr.*, *51*(2), 1045–1053, doi:10.4319/lo.2006.51.2.1045.

Ridgwell, A., and S. Arndt (2015), Why dissolved organics matter: DOC in ancient oceans and past climate change, in *Biogeochemistry of Marine Dissolved Organic Matter*, edited by D. Hansell and and C. Carlson, pp. 1–20, Academic Press, Boston, Mass.

Sexton, P. F., R. D. Norris, P. A. Wilson, H. Palike, T. Westerhold, U. Rohl, C. T. Bolton, and S. Gibbs (2011), Eocene global warming events driven by ventilation of oceanic dissolved organic carbon, *Nature*, *471*(7338), 349–352.

Stuvier, M., and H. Polach (1977), Reporting of ^{14}C data, *Radiocarbon*, *19*(3), 355–363.

Volk, T., and M. I. Hoffert (1985), Ocean carbon pumps: Analysis of relative strengths and efficiencies in ocean-driven atmospheric CO_2 changes, in *The Carbon Cycle Nature Geoscience CO_2: Natural Variations Archean to Present*, pp. 99–110, AGU, Washington, D. C.

Walker, B. D., S. R. Beaupre, T. P. Guilderson, M. D. McCarthy, and E. R. M. Druffel (2016), Pacific carbon cycling constrained by organic matter size, age and composition relationships, *Nat. Geosci.*, *9*(12), 888–891.

Williams, P. M., and E. R. M. Druffel (1987), Radiocarbon in dissolved organic matter in the Central North Pacific Ocean, *Nature*, *330*(6145), 246–248.

Ziolkowski, L. A., and E. R. M. Druffel (2010), Aged black carbon identified in marine dissolved organic carbon, *Geophys. Res. Lett.*, *37*, L16601, doi:10.1029/2010GL043963.